




Research Article

Gingival transcriptomic patterns of macrophage polarization during initiation, progression, and resolution of periodontitis

Octavio A. Gonzalez^{1,2}, Sreenatha S. Kirakodu¹, Linh M. Nguyen³ and Jeffrey L. Ebersole^{3,*} 

¹Center for Oral Health Research, College of Dentistry, University of Kentucky, Lexington, KY, USA

²Division of Periodontology, College of Dentistry, University of Kentucky, Lexington, KY, USA

³Department of Biomedical Sciences, School of Dental Medicine, University of Nevada Las Vegas, Las Vegas, NV, USA

*Correspondence: Dr Jeffrey L. Ebersole, Professor, Department of Biomedical Sciences, Associate Dean for Research, School of Dental Medicine, B221, University of Nevada Las Vegas, Las Vegas, NV, USA. Email: jeffrey.ebersole@unlv.edu

Abstract

Phenotypic and functional heterogeneity of macrophages is clearly a critical component of their effective functions in innate and adaptive immunity. This investigation hypothesized that altered profiles of gene expression in gingival tissues in health, disease, and resolution would reflect changes in macrophage phenotypes occurring in these tissues. The study used a nonhuman primate model to evaluate gene expression profiles as footprints of macrophage variation using a longitudinal experimental model of ligature-induced periodontitis in animals from 3 to 23 years of age to identify aging effects on the gingival environment. Significant differences were observed in distribution of expressed gene levels for M0, M1, and M2 macrophages in healthy tissues with the younger animals showing the least expression. M0 gene expression increased with disease in all but the aged group, while M1 was increased in adult and young animals, and M2 in all age groups, as early as disease initiation (within 0.5 months). Numerous histocompatibility genes were increased with disease, except in the aged samples. An array of cytokines/chemokines representing both M1 and M2 cells were increased with disease showing substantial increases with disease initiation (e.g. IL1A, CXCL8, CCL19, CCL2, CCL18), although the aged tissues showed a more limited magnitude of change across these macrophage genes. The analytics of macrophage genes at sites of gingival health, disease, and resolution demonstrated distinct profiles of host response interactions that may help model the disease mechanisms occurring with the formation of a periodontal lesion.

Keywords: nonhuman primate, aging, macrophage, transcriptome, periodontitis

Abbreviations: BOP: bleeding on probing; IL-10: interleukin 10; PPD: probing pocket depth; PRR: pattern recognition receptors; TLR: Toll like receptor.

Introduction

Periodontitis is a chronic immunoinflammatory lesion of the oral mucosal. A dysbiosis of a complex microbial biofilm containing putative periodontopathogens within the subgingival sulcus drives a persistent inflammatory response that results in destruction of the gingiva, periodontal ligament, and connective tissues, and the underlying alveolar bone [1]. Substantial evidence has documented association of the disease process with various species of bacteria in these pathogenic biofilms [2] and has determined an array of innate immune, inflammatory, and adaptive immune responses that are triggered by these bacteria [3, 4].

Models of the initiation and progression of the disease have emphasized a role of innate responses with alterations in the quality/quantity of the biofilms inducing a neutrophil dominated acute inflammatory response [5, 6]. As the lesion progresses, increasing numbers of mononuclear cells emigrate into the affected tissues, including an array of antigen-presenting cells, e.g. macrophages, reflecting a more chronic inflammatory lesion [7–14]. These cells are particularly adept

at stimulating T cells and regulating the phenotypic features of the T effector cells [15, 16]. The variability in these responses is controlled by both the character of the microbial biofilm stimulus and the host factors in the local microenvironment [17]. Numerous biomarkers of innate immunity are also observed in gingival tissues, e.g. LBP, CD14, TLRs, irrespective of the health of the tissues, although changes in TLR2/TLR4 appear in diseased gingiva [18]. Combined these results support the likely role of macrophages in diseased tissues, and suggest that the development and function of antigen-presenting cells may be crucial in lesion formation and resolution [19].

Current evidence supports an important function for the plasticity of macrophage phenotypes. These varied features include M1 macrophages (classical activation) functioning as an inflammatory cell crucial for protection against microbial challenge [20]. The M2 macrophages (alternative activation) are an immunomodulatory cell generally related to tissue repair and resolution of inflammation [21]. Finally, the M2 macrophage phenotype (deactivated) that is triggered by

IL-10 contributes to tissue remodeling [21–26]. The translation of the range of different stimulatory signals, specifically in response to microbial structures using pattern recognition receptors [20, 27–31], triggers activation, and the phenotype plasticity after engagement of these receptors [32–35]. This process leads to up-regulation of a repertoire of cytokines and chemokines that enable the macrophages to communicate with both B and T cells contributing to local adaptive immune responses [36–41].

The present report describes gingival mucosal tissue responses to evaluate the effects of aging on local expression of a gene footprint of M0, M1, and M2 macrophage phenotypes observed during experimental ligature-induced periodontitis in nonhuman primates. The goal was to provide additional evidence regarding phenotypes of macrophages that occur in clinically healthy tissues and how these change with disease. Additionally, this model enables an exploration of the effects of age on the gingival responses described via the transcriptome analysis.

Methods

Nonhuman primate model and oral clinical evaluation

Rhesus monkeys (*Macaca mulatta*) housed at the Caribbean Primate Research Center (CPRC) at Sabana Seca, Puerto Rico, were used in these studies. Healthy animals were distributed by age into four groups of 9 animals/group for the experimental ligature study ($n = 36$; 19 females and 17 males): ≤ 3 years (Young), 3–7 years (Adolescent), 12–16 years (Adult), and 18–23 years (Aged). The nonhuman primates are typically fed a 20% protein, 5% fat, and 10% fiber commercial monkey diet (diet 8773, Teklad NIB primate diet modified: Harlan Teklad). The diet is supplemented with fruits and vegetables, and water is provided *ad libitum* in an enclosed corral setting.

A protocol approved by the Institutional Animal Care and Use Committee (IACUC) of the University of Puerto Rico, enabled anesthetized animals to be examined for clinical measures of periodontal parameters including probing pocket depth (PPD), and bleeding on probing (BOP) as we have described previously [42]. In this prospective experimental disease study design, the clinical examination included PPD and BOP (0–5 scale). Periodontal health was defined by mean pocket depth ≤ 3.0 mm and mean BOP ≤ 1 (0–5 scale) in a full mouth examination, excluding third molars, and canines examined by a single investigator using a Maryland probe on the facial aspect of the teeth, 2 proximal sites *per* tooth (mesio- and disto-buccal), excluding the canines and third molars. Animals were classified as periodontitis with a mouth mean BOP index of ≥ 2.0 and mouth mean PPD of > 3.0 and were excluded from the study. Following oral screening, the periodontally healthy animals were entered into a standard experimental ligature-induced periodontitis study conducted by the research team [43, 44]. Ligature-induced periodontal disease was initiated as we have previously reported whereby second premolar and first and second molar teeth in all 4 quadrants were ligated by tying a 3-0 non-resorbable silk suture around the cemento-enamel junction of each tooth and using the periodontal probe to position the ligatures below the gingival margin.

Further, clinical evaluation for ligated sites and gingival tissue samples were obtained at 0.5 (initiation), 1 (early progression), and 3 months (late progression). Determination of periodontal disease at the sampled site was documented by assessment of the presence of BOP and PPD of > 4 mm, as we have described previously [43, 44]. Then, ligatures were removed after sampling at 3 months and samples taken 2 months later (resolution) [43, 44]. Since the removal of the ligature eliminates the local noxious mechanical challenge and decreases the microbial burden accumulating at the tooth, this process is similar to nonsurgical periodontal therapy in humans. Previously published histological studies have documented the significant increase in inflammatory cell infiltrate in the ligated tissues consistent with the clinical features of inflammation and increased PPD. While the clinical features show some improvement with disease resolution, as in the human condition, in the previously ligated sites both BOP and PPD remain somewhat elevated compared to baseline values.

Aging comparisons within the study design represent a case-control implementation whereby variations in gene expression were compared to healthy tissue levels within each age group. These variations were then compared across the age groups.

Tissue sampling and gene expression microarray analysis

A buccal gingival sample from either healthy or periodontitis-affected tissue from the premolar/molar regions of each animal was taken at each time point using a standard gingivectomy technique to remove a gingival papillae [45], and maintained frozen in RNA later solution. A single tissue sample was obtained from an individual ligated tooth in each animal ($n = 36$) at each timepoint ($n = 179$ samples). Thus, only ligated teeth (e.g. periodontitis) were sampled and each tooth was only sampled one time during the study. Total RNA was isolated from each gingival tissue using a standard procedure as we have described and tissue RNA samples submitted to the microarray core to assess RNA quality analyze the transcriptome using the GeneChip® Rhesus Macaque Genome Array (Affymetrix) [46, 47]. Individual samples were used for gene expression analyses. Table 1 provides an overview of the $n = 136$ genes whose expression was evaluated in the gingival tissues as related to M0, M1, and M2 phenotype macrophages. These include an array of cytokine/chemokine responses, as well as various cell surface molecules that provide some discrimination among these phenotypes.

Data analysis

The expression intensities across the samples were estimated using the Robust Multi-array Average (RMA) algorithm with probe-level quintile normalization, as implemented in the Partek Genomics Suite software version 6.6 (Partek, St. Louis, MO). The differential expression was initially compared using one way ANOVA across time points within an age group. For genes that had significant mean differences, two sample *t*-tests were used to investigate differences comparing baseline healthy to disease and resolution samples. Statistical significance was considered by a *P*-value < 0.05 . Correlation analyses across the Ig genes were determined using a Pearson Correlation Coefficient with a *P*-value < 0.001 .

Table 1: Macrophage genes examined using Affymetrix *M. mulatta* gene probes

Probe ID	Gene Symbol	Mφ phenotype	Probe ID	Gene symbol	Mφ phenotype
13670191	CD68	M0	13703388	PLA1A	M1
13766692	CD11b	M0	13728299	PSMA2	M1
13745458	MAMU-DRB1	M0	13739428	PSMB9	M1
13745450	MAMU-DQB1	M0	13783047	PSME2	M1
13745514	MAMU-DMB	M0	13714209	PTX3	M1
13745524	MAMU-DMA	M0	13660496	SLC2A6	M1
13745532	MAMU-DOA	M0	13666399	SLC31A2	M1
13814368	MAMU-DOB	M0	13822238	SLC7A5	M1
13745539	MAMU-DPA	M0	13722177	SOCS1	M1
13739456	MAMU-DPB	M0	13681736	SOCS3	M1
13817328	MAMU-DQA1	M0	13674865	SPHK1	M1
13814540	MAMU-DRA	M0	13635204	STAT1	M1
13703531	CD86	M0	13754131	TLR2	M1
13756250	CXCL13	M0	13754834	TLR3	M1
13768578	CD14	M0	13666203	TLR4	M1
13824962	BCL2A1	M1	13755606	TLR6	M1
13651625	BIRC3	M1	13739126	TNF	M1
13671791	CCL11	M1	13786822	TRAIL/TNFRSF10A	M1
13678304	CCL15	M1	13801311	ADK	M2
13662586	CCL19	M1	13676169	ALOX15	M2
13671776	CCL2	M1	13749204	ARG1	M2
13632412	CCL20	M1	13788523	CA2	M2
13678315	CCL3	M1	13671796	CCL13	M2
13813554	CCL3L1	M1	13719231	CCL17	M2
13814596	CCL4L1	M1	13671907	CCL18	M2
13678276	CCL5	M1	13678304	CCL23	M2
13671791	CCL8	M1	13727629	CCL24	M2
13712469	CCR2	M1	13600605	CD16/FCGR3	M2
13679479	CCR7	M1	13623027	CD163	M2
13610718	CD40	M1	13709768	CD200R	M2
13709961	CD80	M1	13697742	CD209	M2
13615329	CERK	M1	13820542	CD23/FCER2	M2
13751757	CXCL10	M1	13588134	CD32/FCGR2	M2
13751751	CXCL11	M1	13735835	CD36	M2
13751763	CXCL9	M1	13585973	CHI3L2	M2
13636236	CXCR1	M1	13623249	CLEC7A	M2
13615586	ECGF1/TYMP	M1	13658225	CTSC	M2
13797146	FAS	M1	13641372	CXCR4	M2
13664166	GADD45G	M1	13636114	FN1	M2
13601504	HSD11B1	M1	13830596	HEXB	M2
13787604	IDO1	M1	13608692	HMOX1	M2
13816188	IFNA13	M1	13710643	HRH1	M2
13663023	IFNA2	M1	13755205	HS3ST1	M2
13663057	IFNB1	M1	13627601	IGF1	M2
13626341	IFNG	M1	13589121	IL10	M2
13769388	IL-12A	M1	13640715	IL1R2	M2
13753798	IL15	M1	13641271	IL1RN	M2
13799623	IL15RA	M1	13683683	KLF5	M2
13645870	IL1A	M1	13608939	MAFF/v-maf	M2
13645879	IL1B	M1	13682112	MAFG/v-maf	M2
13640727	IL1R1	M1	13794909	MRC1L1	M2
13618605	IL23A	M1	13790532	MSR1	M2
13759870	IL7R	M1	13648363	MS4A4A	M2
13735121	IL6	M1	13648365	MS4A6A	M2
13756408	IL8	M1	13707572	P2RY14	M2
13730418	IRF5	M1	13710601	PPARG	M2

Table 1. Continued

Probe ID	Gene Symbol	Mφ phenotype	Probe ID	Gene symbol	Mφ phenotype
13669029	NFIL3	M1	13787096	SCARA3	M2
13752893	NFKB1	M1	13613519	SCARF2	M2
13783533	NFKBIA	M1	13766153	SEPP1	M2
13677579	NOS2	M1	13679882	STAT3	M2
13621445	OAS1	M1	13625948	STAT6	M2
13621462	OAS2	M1	13700499	TGFB1	M2
13736094	PBEF1/NAMPT	M1	13708591	TGFBR2	M2
13794590	PFKFB3	M1	13755600	TLR1	M2
13794461	PFKP	M1	13588675	TLR5	M2

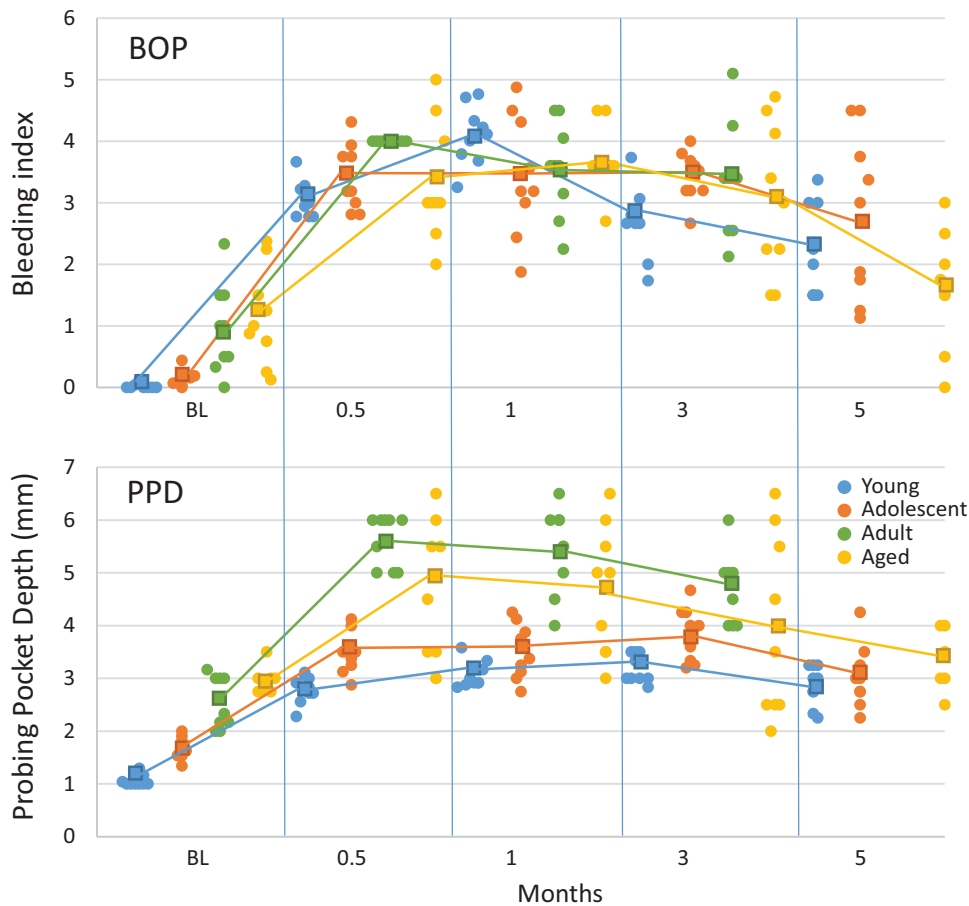


Figure 1: Clinical features (BOP, bleeding on probing; PPD, probing pocket depth) of disease in the young, adolescent, adult, and aged groups of animals. Each point denotes an individual animal at each time point. The squares denote the group means.

One-way ANOVA ($\alpha = 0.05$) was used to identify genes from this set that were differentially expressed in health or disease for at least one of the age groups. Given the sample-size limitations in the present study and subtle transcriptional response in the current experimental setting, no multiple-testing correction to control for false-discovery or family-wise error were imposed in the differential gene expression analysis.

Gene expression data of the 136 macrophage genes (15 M0, 72 M1, 49 M2) and 179 monkey samples were normalized on the scale of: M0 (0.0188–0.608), M1 (0.00610–0.242), and M2 (0.00610–0.360). In each normalized scale pair, the

lowest data value was set at the lower number and the highest data value was set to the higher number. The data normalization, heatmaps, and dendrograms for the cluster analyses were generated using BioVinci software (BioTuring Inc.).

Results

Health-related transcriptomic patterns of macrophage gene expression affected by age

Figure 1 displays the clinical measures in younger and older animals following ligature-induced periodontitis. Of note was the extensive and more prolonged inflammatory response

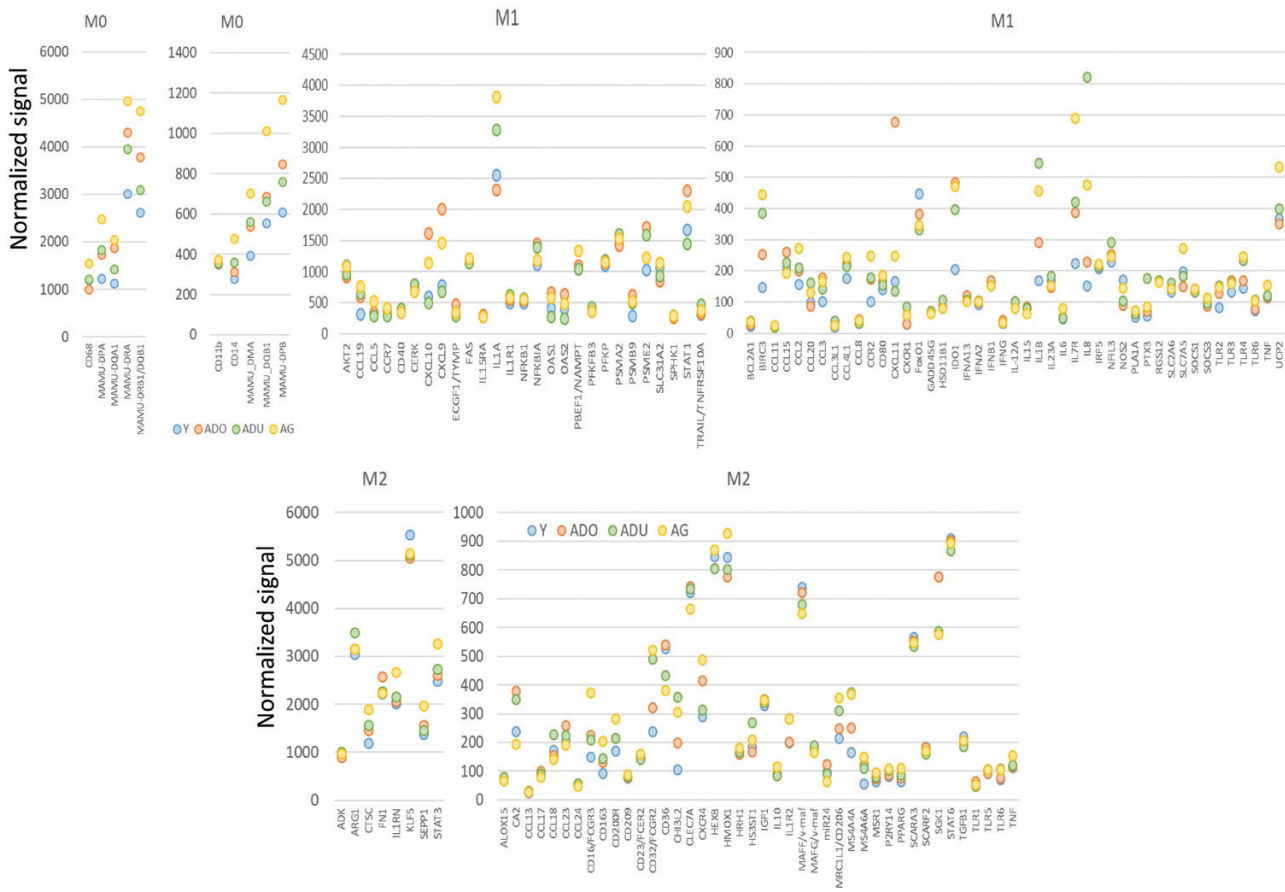


Figure 2: Normalized counts for gene expression of macrophage genes in healthy gingival tissues from the 4 age groups. The dots denote the mean expression level in each age group

(BOP) in the younger animals, albeit significantly lower tissue destruction measures (PPD) were observed in this group. Also, some variation in presentation of the disease measures was seen in animals within each age group.

Figure 2 provides a summary of the expression of groups of genes with patterns indicative of M0, M1, or M2 macrophages in healthy gingival tissues from different age groups of animals representing from about 10 to 80 year old human subjects. With the M0 genes, generally, lower expression levels were seen in the youngest group and the aged group demonstrated the most elevated expression across these genes. The greatest expression of M1 genes included CXCL9, CXCL10, IL1A, PSMA2, PSME2, STAT1, BIRC3, IDO1, IL1B, IL7R, and IL8 that were significantly differ across the age groups ($P < 0.05$). Baseline healthy M2 gene expression did not appear to define a particular pattern related to age. While the majority of the M2 genes showed great similarity in levels across the age groups, expression of ARG1, CTSC, FN1, IL1RN, KLK5, SEPP1, and STAT3 was significantly greater ($P < 0.05$) than other M2 genes.

Transcriptomic patterns of macrophage gene expression in disease initiation, progression, and resolution

Figure 3 provides an overview of the gene footprint changes for M0, M1, and M2 cell expression in the gingival tissues with disease and resolution in the various age groups. While

there were some difference in macrophage gene expression profiles in health, it was anticipated that more extensive changes would occur with an ongoing disease process. Expression of M0 related genes in the gingival tissues generally exhibited some changes in the young and adolescent animals that increased with disease progression and then decreased at resolution. Smaller changes were noted in the adult and aged groups, with gene expression in the aged animals showing a similar level throughout all the time points. The greatest change in M1 gene expression occurred in the adult animals at disease initiation (0.5 months). Both adolescent and aged animals showed little change, with potentially a small decrease throughout the disease and resolution. The samples from young animals also showed an increase in gene expression with disease initiation that remained above healthy levels throughout the disease process. These findings contrasted with the M2 gene expression patterns that increased substantially in all age groups with disease initiation. Levels of these phenotype genes remained elevated in only the young animals at resolution, while the other age groups generally returned to levels in healthy tissues. Figures 4–6 provides a slightly different view of the potential interaction of these macrophage phenotypes within the gingival tissues. This analysis was based upon the perspective that the relative levels of M0, M1, and M2 functions, as expressed by changes in mRNA levels, would be an important descriptor of the gingival environment at the individual animal level in health and disease. The patterns in Fig. 4 show relatively consistent levels of M1

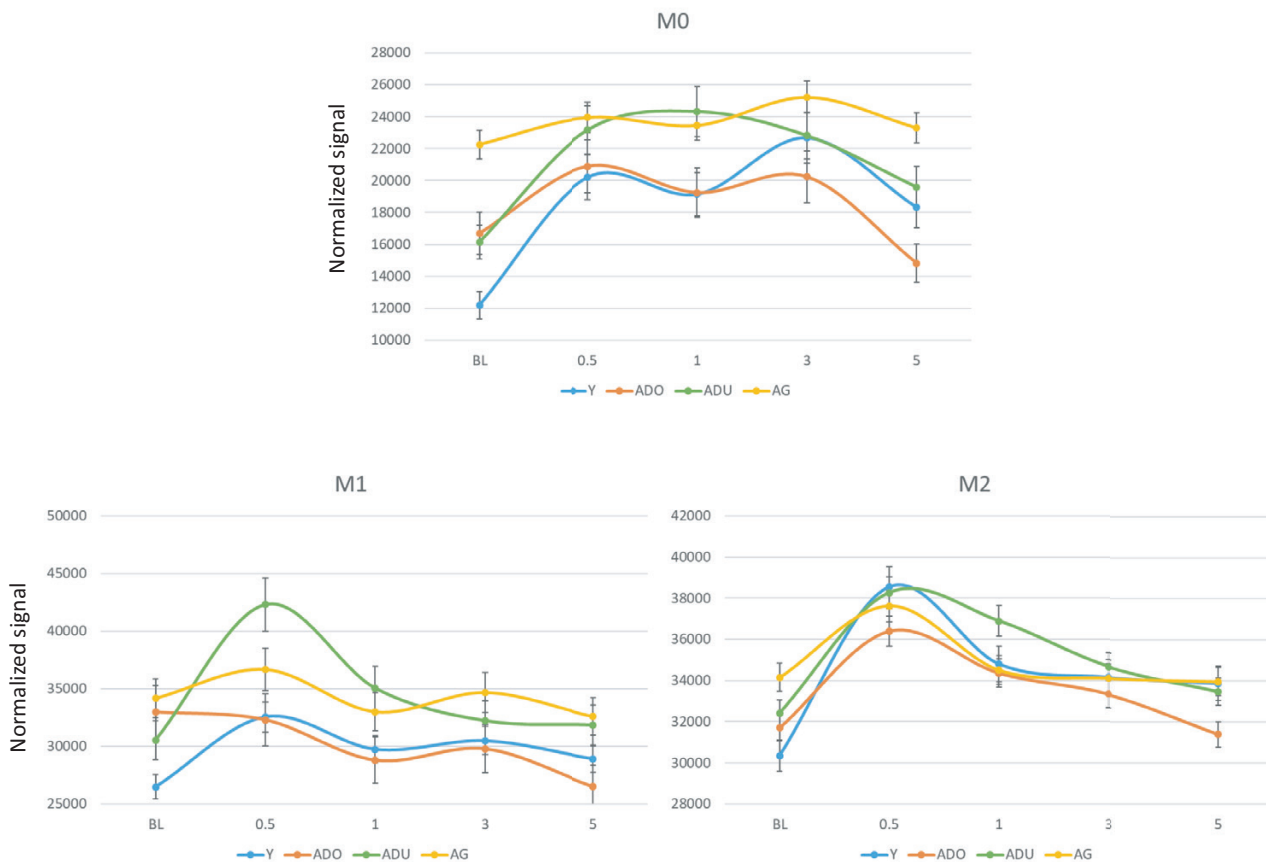


Figure 3: Summation of expression for genes denoting M0, M1, and M2 macrophages.

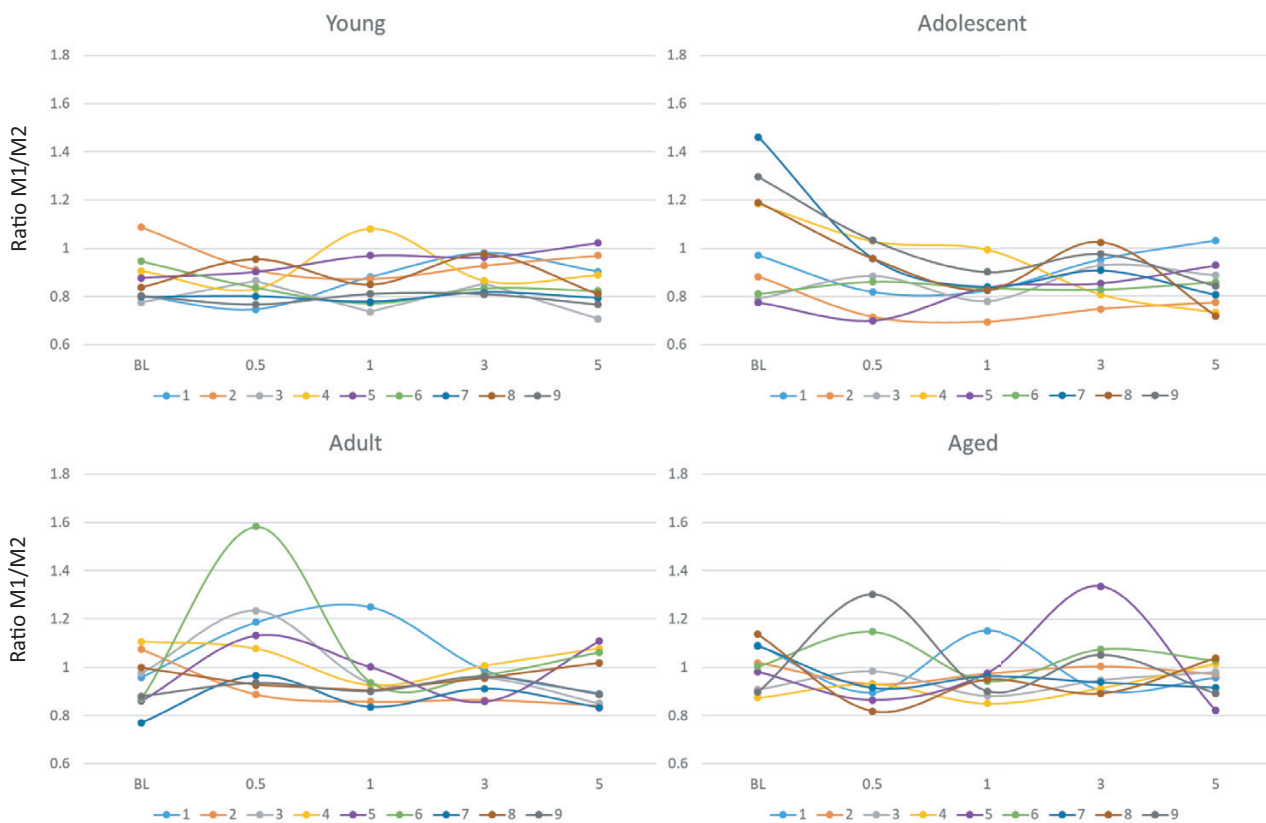


Figure 4: Summation of expression for genes. The points denote group means and the vertical brackets enclose 1 SD. Summaries of the ratio of expression levels for M1/M2 are presented with each point denoting the ratio for each individual animal in all groups at all time points.

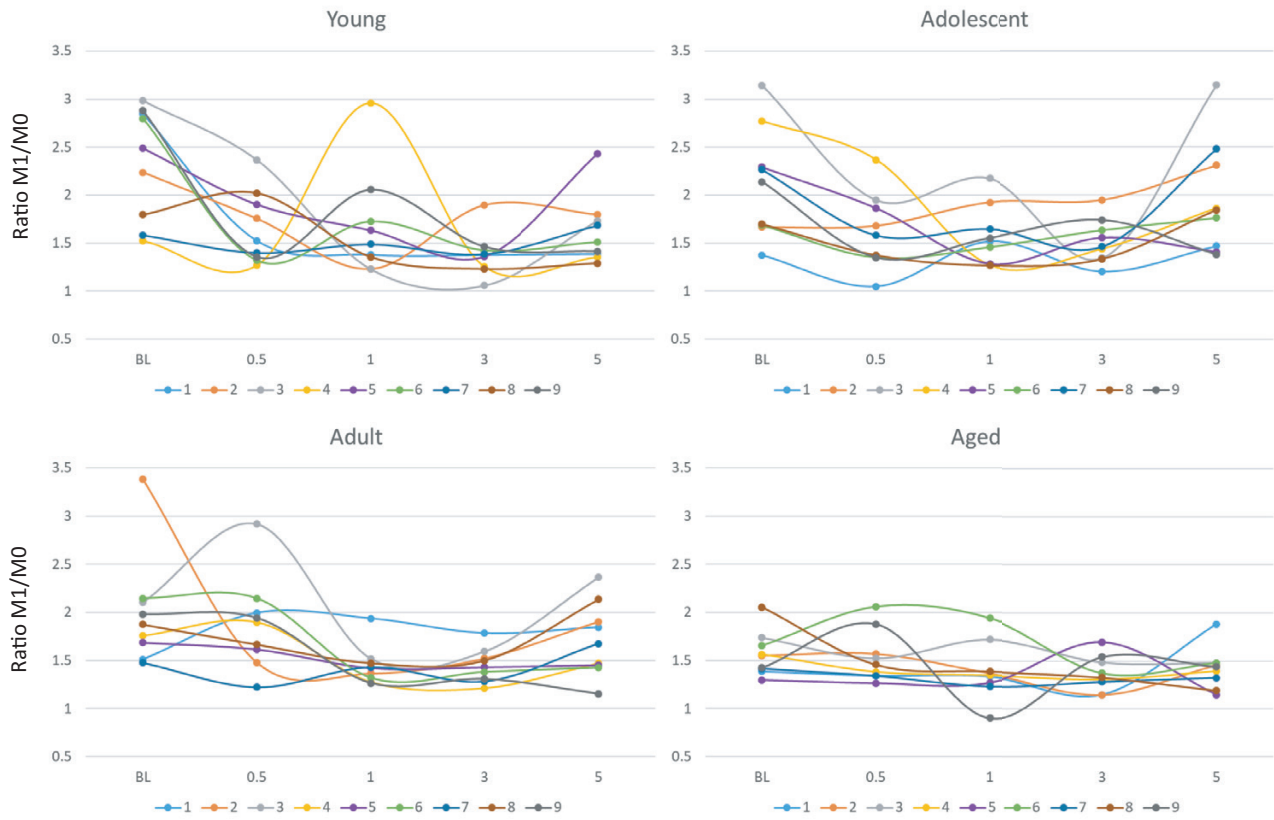


Figure 5: Summation of expression for genes. The points denote group means and the vertical brackets enclose 1 SD. Summaries of the ratio of expression levels for M1/M0 are presented with each point denoting the ratio for each individual animal in all groups at all time points

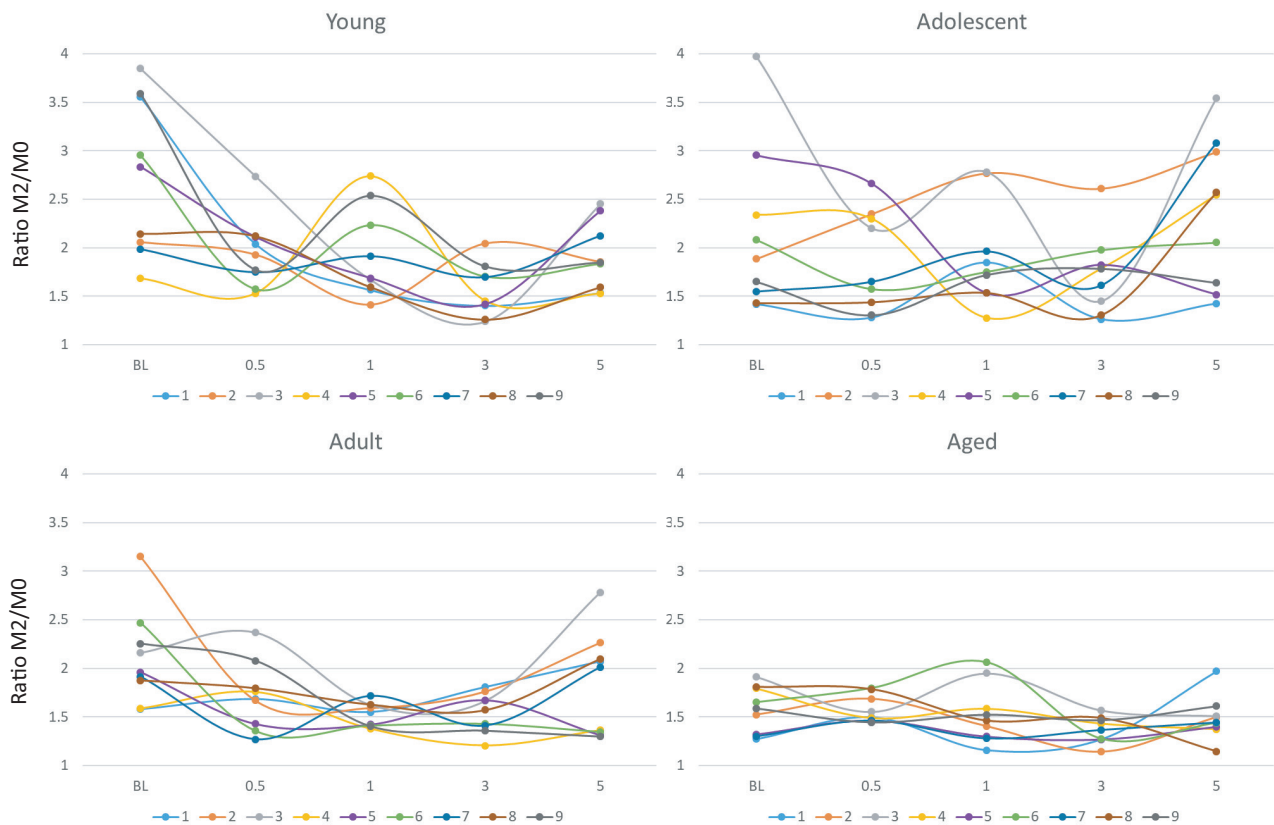


Figure 6 : Summation of expression for genes. The points denote group means and the vertical brackets enclose 1 SD. Summaries of the ratio of expression levels for M2/M0 are presented with each point denoting the ratio for each individual animal in all groups at all time points.

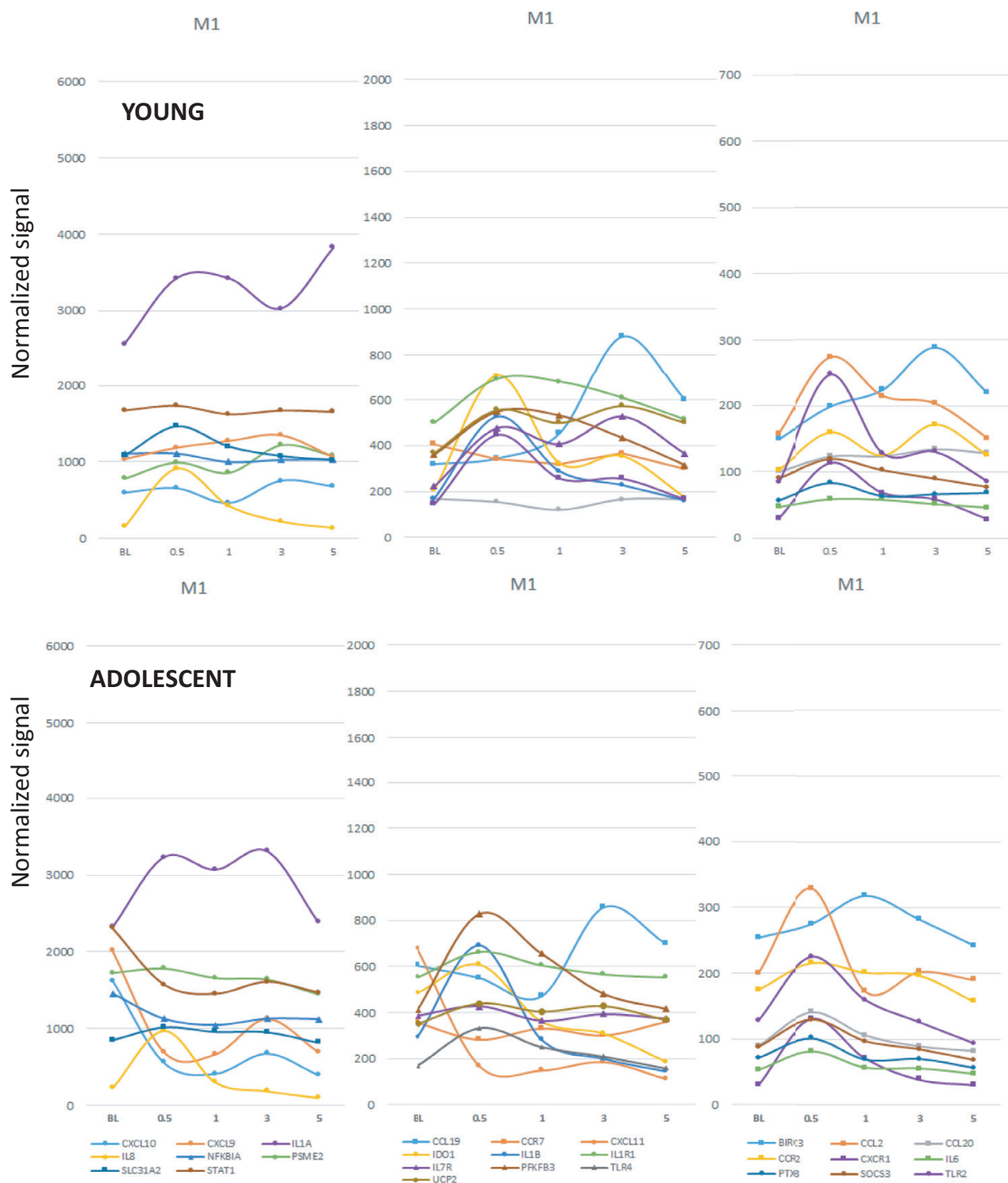


Figure 8: Gene expression changes in the various age groups for M1 macrophages. The points denote the group means of the normalized signals. Of the 136 total genes, only those demonstrating a change of ≥ 1.5 between any two time points in any of the age groups are included.

increase ($P < 0.05$) to peak levels during progression. More substantial changes in the M1 genes was noted in the adult samples, with multiple genes that had showed some change in the younger groups now demonstrating substantial increases in adults with peak levels as early as disease initiation (Fig. 9). Additionally, TLR4, PTX3, SOCS3, CCL20, and CCR2

all showed significant increases ($P < 0.05$) in adults at disease initiation. IL1A and CCL19 were significantly increased ($P < 0.05$) throughout disease and even in resolution samples. As was noted with M0 genes, changes in M1 gene expression appeared to be tempered in the aged samples. Nevertheless, there were similarities in differential expression profiles in the

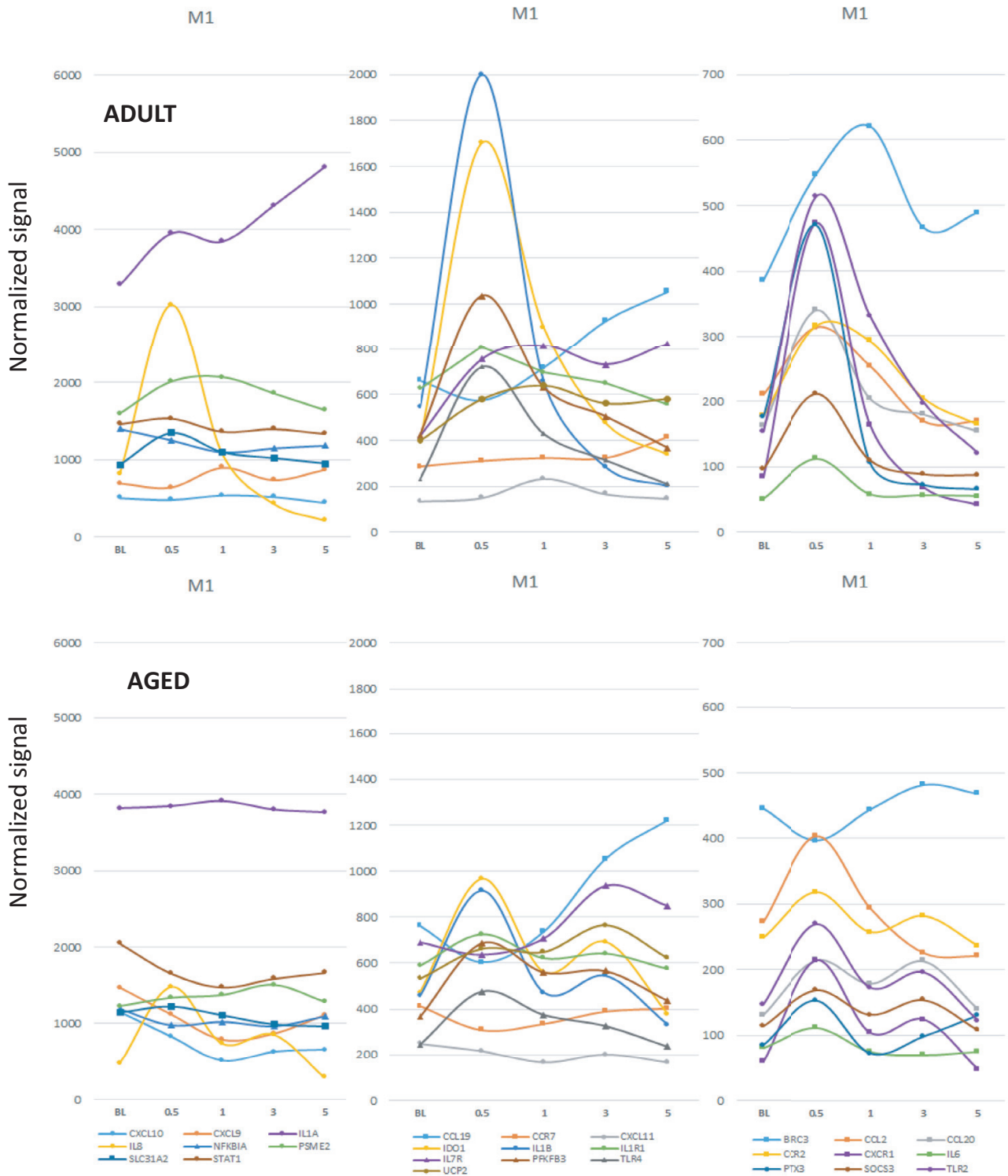


Figure 9: Gene expression changes in the various age groups for M1 macrophages. The points denote the group means of the normalized signals. Of the 136 total genes, only those demonstrating a change of ≥ 1.5 between any two time points in any of the age groups are included.

aged animals of IL8, IL1B, IDO1, CCL19, CXCR1, and TLR2 ($P < 0.05$ vs. baseline) to the adult tissues.

Of interest was that in the young and adolescent animals, there were significant increases in M2 gene expression levels particularly with disease initiation, and then decreasing during progressing disease (Figs. 10 and 11). A similar pattern

was noted in the adult and aged samples related to M2 gene expression increases with disease initiation. In the adults, striking features were increases in CD32, CD36, CD163, and MS4A6A compared to the other groups. Additionally, CCL18, CA2, and CD16 were substantially increased at disease initiation in the adolescent, adult, and aged samples.

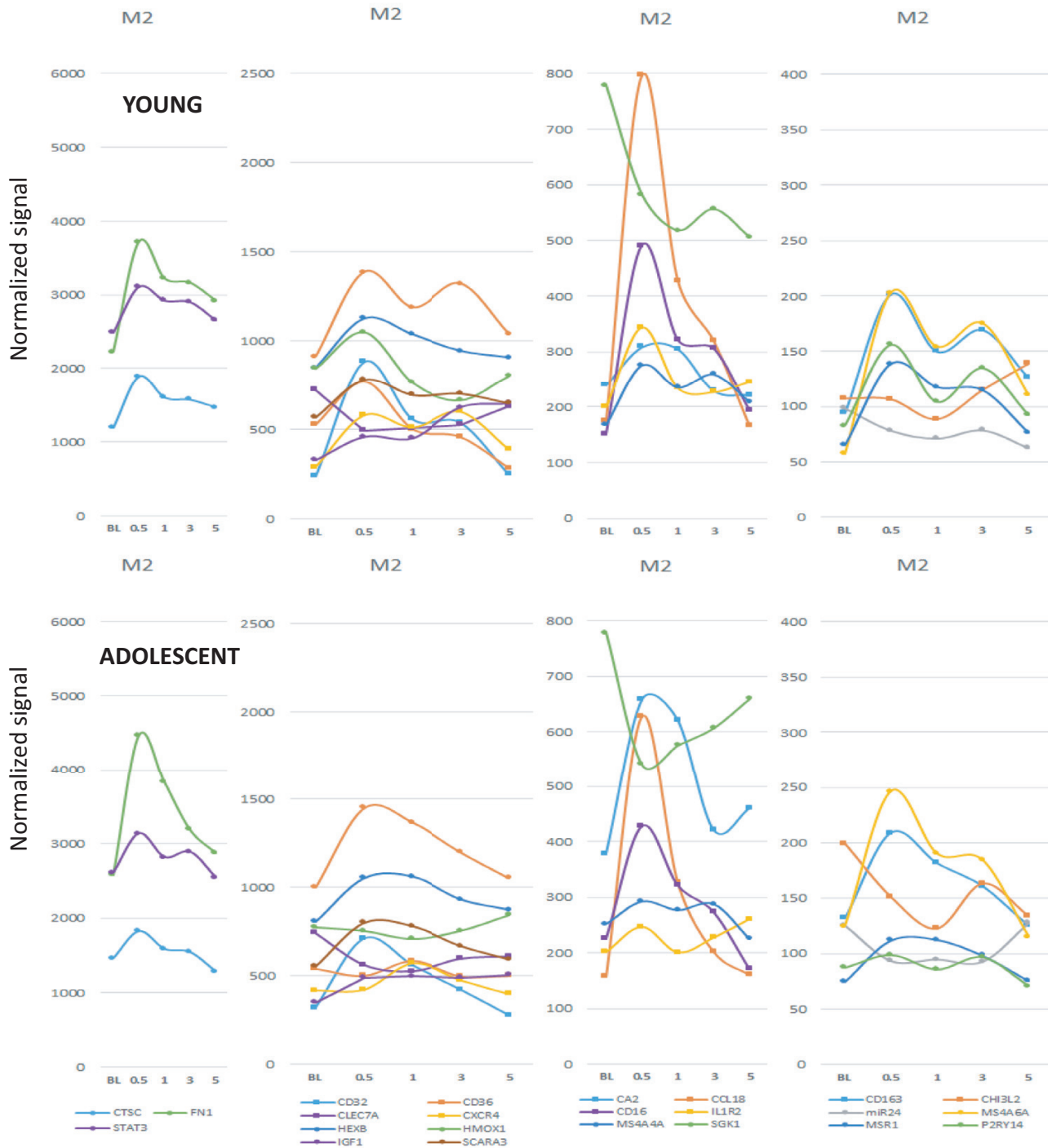


Figure 10: Gene expression changes in the various age groups for M2 macrophages. The points denote the group means of the normalized signals. Of the 136 total genes, only those demonstrating a change of ≥ 1.5 between any two time points in any of the age groups are included.

Also observed was a somewhat unique profile for CHI3L2 (Chitinase 3-like 2) with elevated levels in health, decreasing during the initial 0.5 months with disease initiation in these same age groups.

Figures 12–13 provides a summary comparison of the M0, M1, and M2 gene expression across age groups and in health, disease, and resolution. This analysis used a z-score normalization within a gene including all ages and time points. Generally, the M0 gene expression was lower in

healthy tissues for all age groups. The expression increased during disease, with somewhat higher levels by 3 months of disease progression. In the resolution samples, the M0 genes decreased in all age groups.

The M1 genes were routinely lower in the healthy samples from young and adult animals. An array of ~15–20 M1 genes showed increased levels in the healthy samples from the adolescent animals. During disease, the majority of the M1 genes increased in all age groups, with the greatest

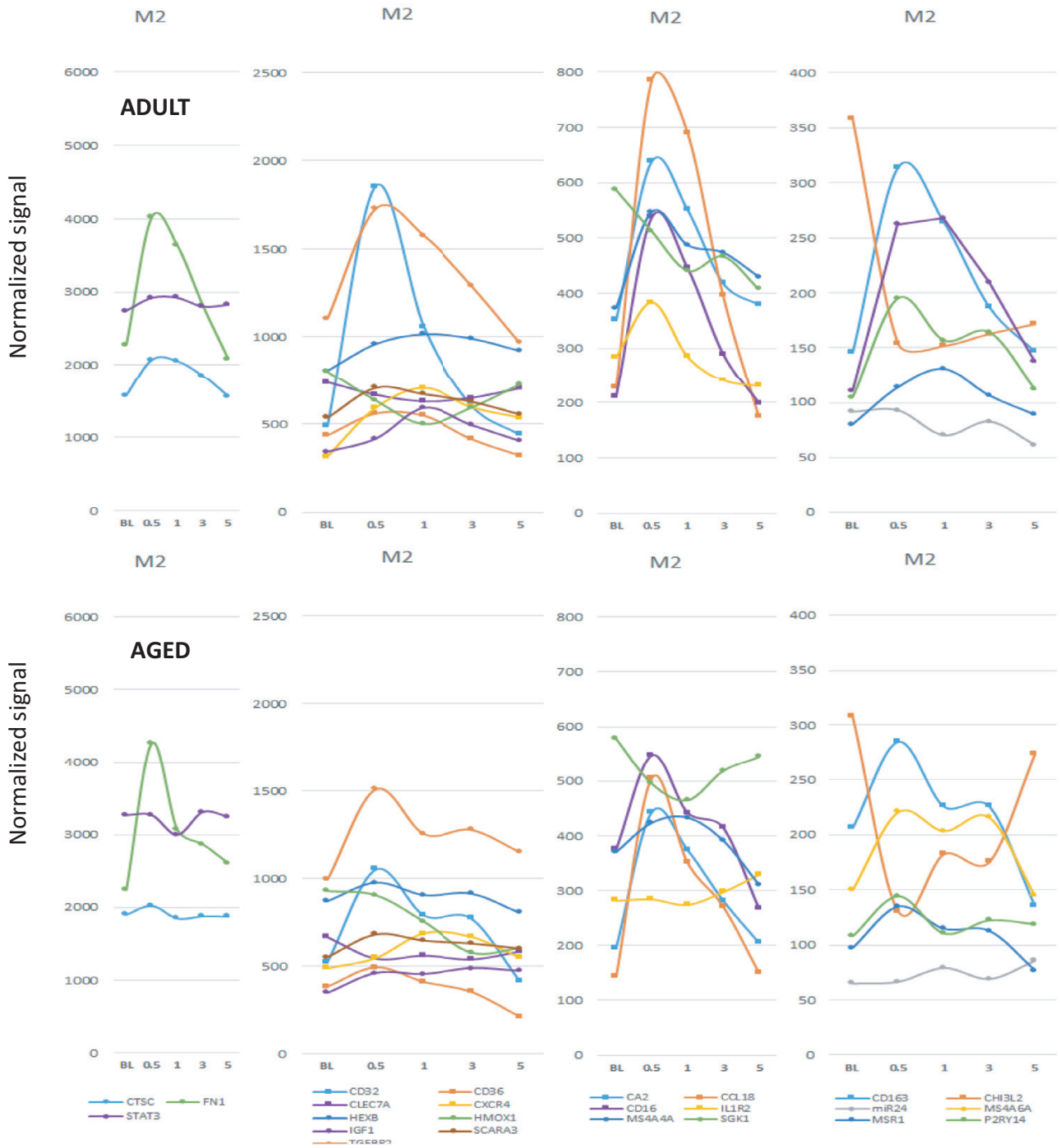


Figure 11: Gene expression changes in the various age groups for M2 macrophages. The points denote the group means of the normalized signals. Of the 136 total genes, only those demonstrating a change of ≥ 1.5 between any two time points in any of the age groups are included.

increases noted in the disease initiation (2 weeks) specimens and decreasing with progressing disease. The magnitude of this change was most striking in the adult disease samples. As with the M0 genes, this array representing M1 cells showed relatively decreased expression in all age groups in the resolution samples.

Figure 13 demonstrates the relative expression of M2 genes in the samples. Generally, lower levels were seen in healthy tissues in all age groups, most notable in the young and adult samples. As was noted with M1 genes, by 0.5 months with

disease initiation, a wide array of M2 genes showed elevated expression levels in all age groups. The frequency/levels tended to decrease with progressing disease in the young, adolescent, and aged animals. By 5 months with clinical resolution, the M2 genes were lower in all age groups.

Figures 14–16 depict a heatmap of cluster analyses of the M0, M1, or M2 gene expression profiles for all the individual samples from animals in each age group and at each time point in the protocol. The results shows 9 clusters of samples based upon the profile of M0 genes (Fig. 14), 11 clusters

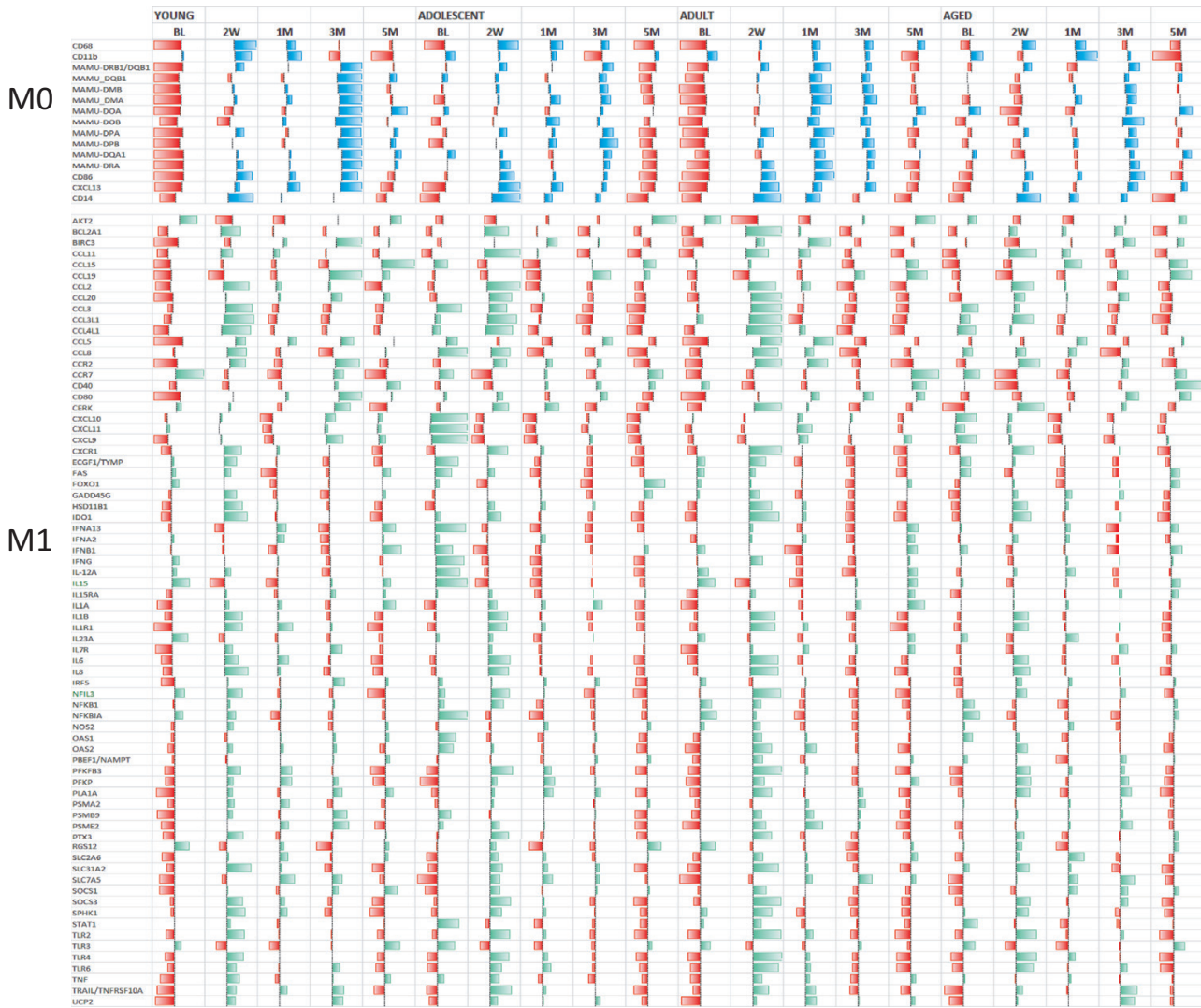


Figure 12: Depiction of the z-score normalization of gene expression for all M0 and M1 genes. The z-scores were determined within a gene across all age groups and time points. The bars denote group means at the time point. The larger the bar (left of center decreased and right of center elevated expression), the greater the difference of the z-scores for gene expression.

for the M1 genes (Fig. 15), and 9 clusters for the M2 genes (Fig. 16). The patterns predict variation in the gene expression patterns across the samples and suggested potentially somewhat distinct profiles across the macrophage phenotype genes. Interrogating the identifiers for each of the samples demonstrated the cluster patterns presented in Figs. 17–19. Summarizing the patterns indicated that while there were differences in clusters within the healthy, diseased, and resolution samples across the age groups, major differences in sample clusters were specifically related to the age of the animals with the M0 and M1 clusters. However, the sample grouping with the M2 clusters appeared to present differences driven by both age and the disease status of the samples.

Transcriptomic patterns of macrophage gene expression associated with clinical features of disease

The macrophage-related gene expression patterns were also evaluated related to individual animal clinical parameters of inflammation (BOP) and tissue destruction (PPD) in this

periodontitis model (Fig. 20). In this analysis significant correlations in individual M0, M1, or M2 genes with the clinical measures in each animal were tabulated, including both positive and negative correlations. Generally, the M0 correlations with both BOP and PPD were skewed toward a positive relationship in both younger and older animals and was the most pronounced in health and resolution samples. M1 genes showed generally positive correlations with both BOP and PPD in healthy samples in both age groups, while the frequency of correlations were positive and somewhat elevated related to BOP in diseased samples from the older group. Resolution samples showed the highest correlations of M1 genes with both BOP and PPD in the older animals. Finally, M2 genes showed a higher frequency of correlations in the older samples with disease and resolution.

Discussion

A summary of the literature demonstrates that macrophages are present in the periodontium and respond to the local

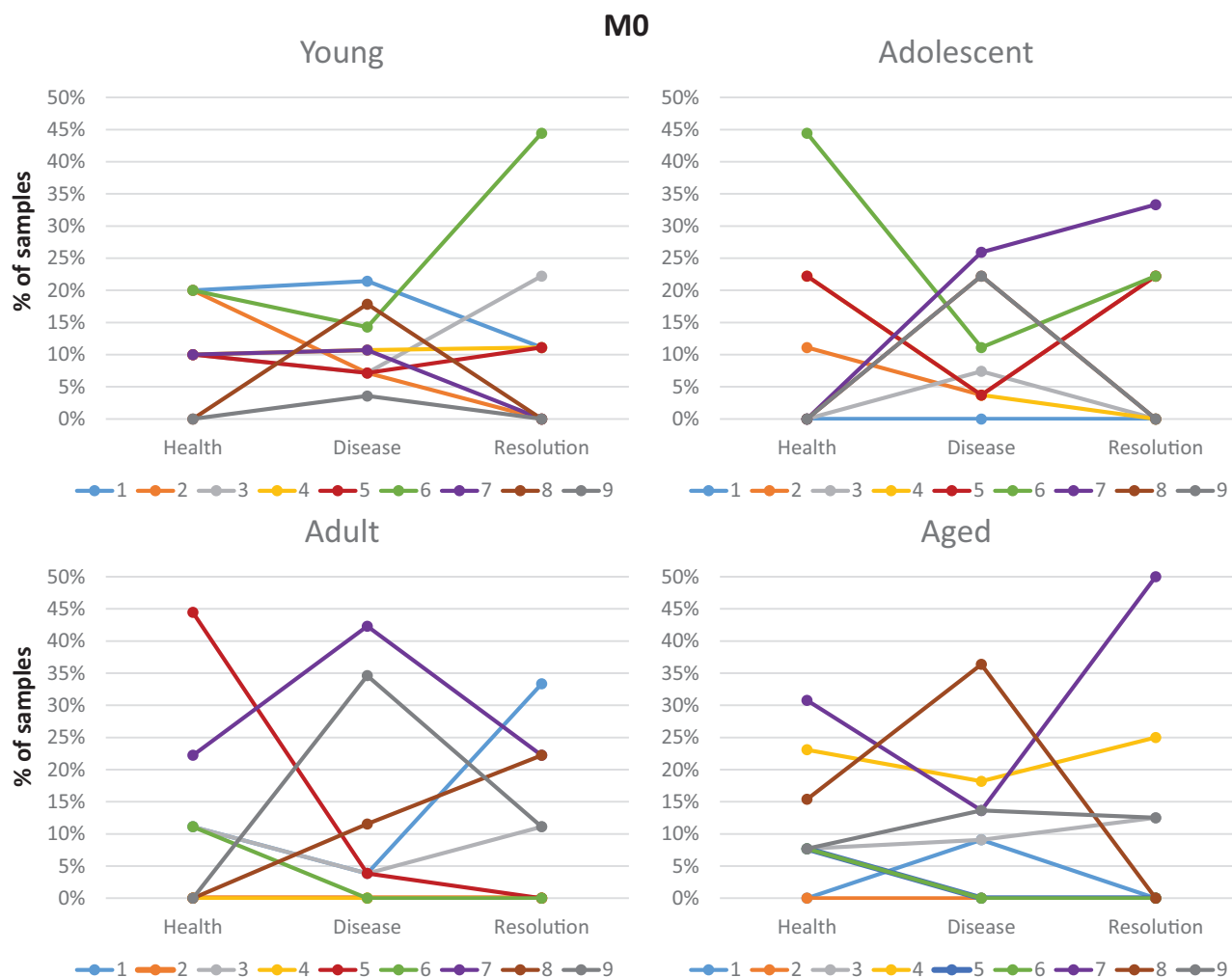


Figure 17: Summary of the distribution of samples within the M0 cluster. The points denote the percentage of samples within the age group at each time point that were contained within the specific gene expression cluster.

disease and resolution. M1 gene expression changes in disease were lower in the younger groups, elevated in adult samples, and minimized in the aged gingival tissues. In contrast, there were significant increases in M2 gene expression levels particularly with disease initiation, and then decreasing during progressing disease across all the age groups. Of interest were the relationships between genes for macrophage phenotypes and the disease presentation of the animals. Some clear differences were noted in younger vs. older animal samples, with both M1 and M2 genes related to BOP and PPD levels. While these measures did not show extensive variation in healthy tissues, the M0 genes showed a high frequency of correlations with the clinical features. While this is a longitudinal model of disease, whether the changes in macrophage phenotype footprints reflect other parameters driving the disease process, or actually contribute to the tissue changes cannot be discerned from these data. Nevertheless, in this controlled disease model, there was reasonable evidence that the macrophages have some role in the transition from health to disease and likely back to resolving the lesion [43]. However, as we have reported with regard to gene expression profiles for other biologic pathways in mucosal tissues [44, 47, 54, 55], while aged gingival tissues appear clinically healthy, the tissues seem to reflect an altered local environment of cellular

responses and likely associated functions that may predispose to an enhanced likelihood of a future tissue destructive process. In periodontitis tissues, increases in total gene expression presumably reflected an increase in the macrophage populations in the tissues, particularly with disease initiation. This appeared to be related to a magnitude of increase in gene expression associated with M1 cells, although, the M2 gene signals were increased in all age groups at this time point. Thus, as has been reported previously [48], the balance of these cells within the periodontal tissues are likely crucial for maintaining or re-establishing homeostasis or contributing to the dysregulated inflammatory response in disease. Moreover, aging clearly has an impact on the capacity to maintain an appropriate balance of functions in these mucosal tissues.

Focusing on the major gene response changes in the tissues identified highlights of the transcript changes related to macrophage biology. With M0 cells, MAMU-DRA, -DRB1, -DPB, -DMA, and DQB1 were all elevated during disease, with most pronounced changes in young and adult animals. Of interest is that with the aged group, these histocompatibility antigens were minimally changed suggesting a potential for decreased maturation of adaptive immune responses. This is consistent with our recent report regarding the decreases in immunoglobulin gene diversity in the periodontal

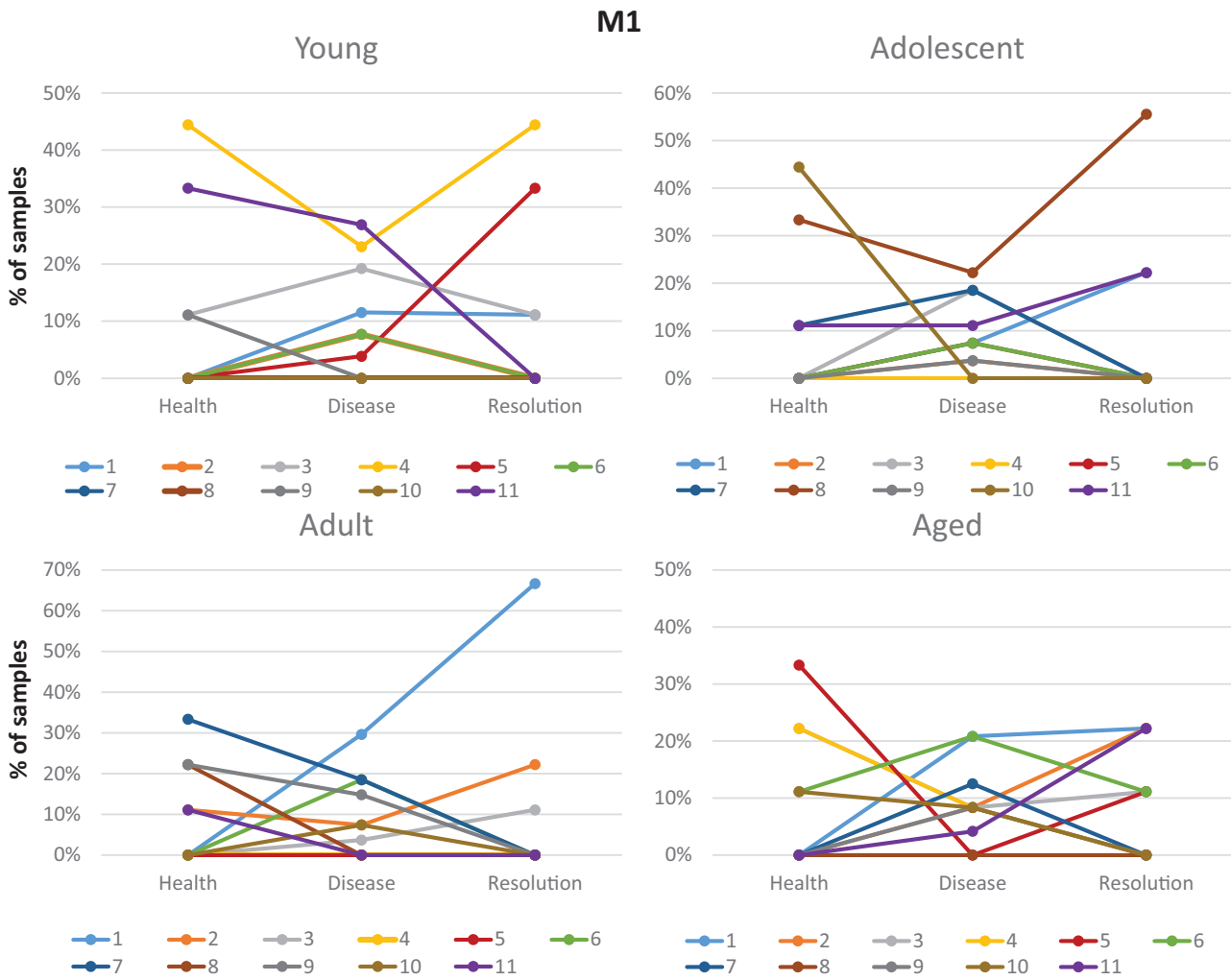


Figure 18: Summary of the distribution of samples within the M1 clusters. The points denote the percentage of samples within the age group at each time point that were contained within the specific gene expression cluster.

tissues of aged animals [56]. Additionally, CXCL13 (B cell chemoattractant) and CD14 (LPS coreceptor) were increased with disease in all age groups related to both innate and adaptive immune responses.

The transcripts for M1 genes that were most impacted by the disease process included two major PAMPS, TLR2, and TLR4 that were both upregulated with disease, supporting the potential for greater cellular interaction with the evolving microbiome. This was coupled with increases in gene expression of chemokines CXCL8 (neutrophils), CCL19 (T and B cells), CCL2 (monocytes), and CCL20 (dendritic, T and B cells), as well as the CCR2 (CCL2 ligand) and CXCR1 (IL8 ligand) receptors signaling a change in the local environment related to increased inflammatory cell emigration into the inflamed tissues. Both IL1A and IL1B were up-regulated representing major pro-inflammatory cytokines. However, we also observed major changes in expression of IDO1 (indoleamine 2,3-dioxygenase) that helps maintain homeostasis by preventing autoimmunity or immunopathology, BIRC3 (Baculoviral IAP Repeat Containing 3) that regulates caspases and apoptosis, contributing to modulating inflammatory signaling and immunity, and PTX3 (pentraxin 3) that regulates innate

resistance to pathogens and inflammatory reactions. Thus, the features of the classically activated macrophages represent dynamic interactions to populate the inflammatory tissues to cope with the microbiome changes, but also demonstrate factors that are produced to help control the generation of the inflammatory responses.

Attributes of the M2 responses showed a consistent increase in genes related to immune response including CTSC (cathepsin C) that activates serine proteases that can contribute to immune protection. Also, CCL18 (lymphocyte chemoattractant) is produced by innate immune system to act on adaptive immune responses with two immunoglobulin receptors, CD32 (Fcγ receptor 2A) and CD16 (Fcγ receptor 3A) up-regulated with disease initiation. Additionally a number of M2 scavenger receptors are rapidly increased including CD36 (thrombospondin, fibronectin, collegan, amyloid beta), CD163 a major acute phase-regulated receptor on M2 cells, and both MS4A6A (Membrane Spanning 4-Domains A6A) for signal transduction from a multimeric receptor complex and MS4A4A (Membrane Spanning 4-Domains A4A) that essential for dectin-1-mediated activation of macrophages. Two additional consistent M2-associated changes included CA2 (carbonic anhydrase 2) that is needed for bone resorption

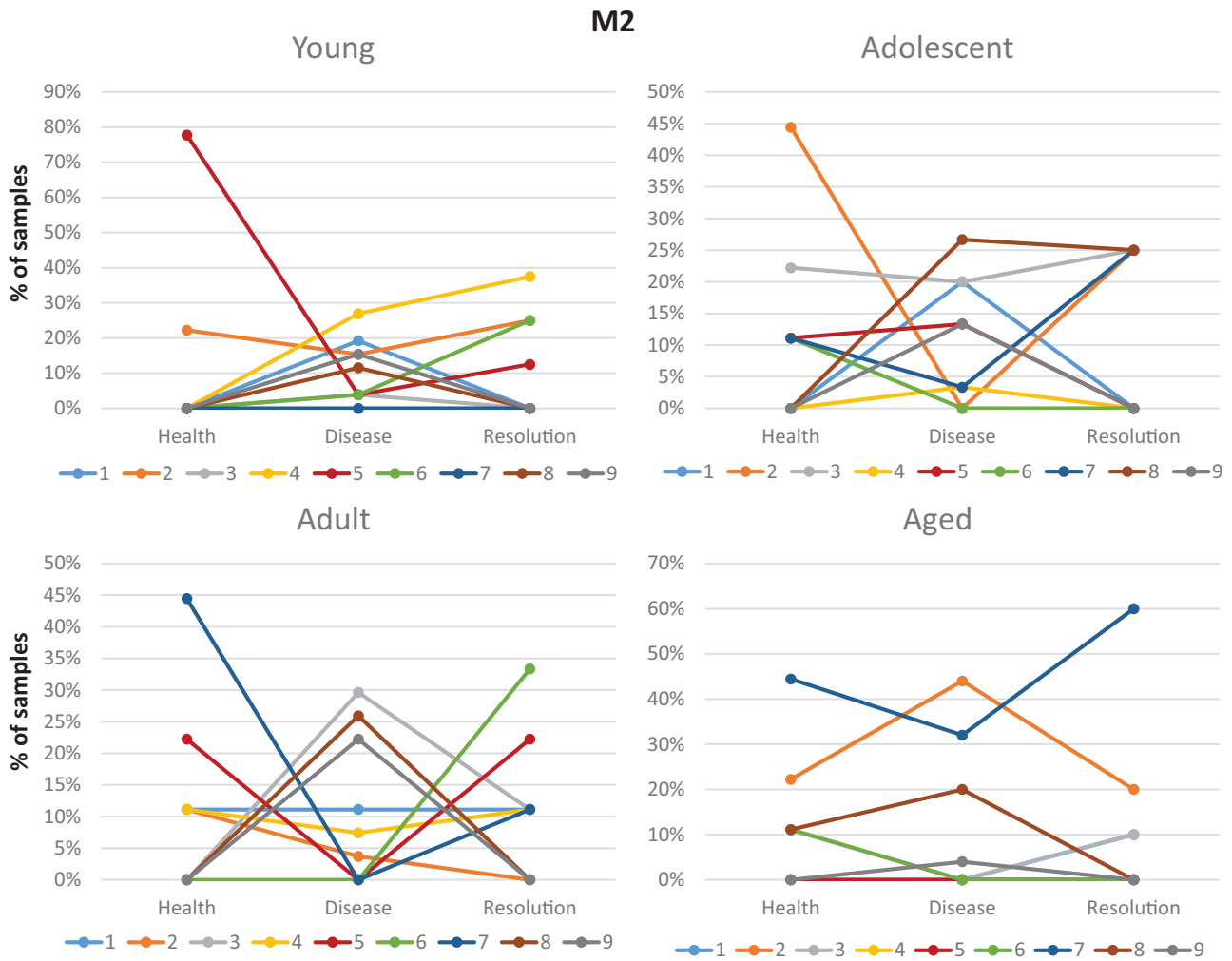


Figure 19: Summary of the distribution of samples within the M2 clusters. The points denote the percentage of samples within the age group at each time point that were contained within the specific gene expression cluster.

and osteoclast differentiation and FN1 (fibronectin 1) that is critical for cell adhesion and wound healing. These results suggested a role for the M2 cells in attempting to re-establish some level of homeostasis in the tissues. However, this contrasts with HMOX1 (heme oxygenase 1), which is anti-inflammatory, SGK1 (Serum/Glucocorticoid Regulated Kinase 1) that has an important role in cellular stress by regulating inflammatory responses, and CHI3L2 (Chitinase 3 Like 2) that is induced to regulate inflammation that were all substantially decreased with disease initiation and progression. While there is limited information of these molecules in periodontitis, of interest, HMOX1 has been shown to be increased in gingival tissues of smokers [57] compared to healthy or periodontitis tissues. SGK1 promotes M2 activation via regulation of FOXO1 and STAT3 and appears to be a central regulatory molecules with *Porphyromonas gingivalis* induced inflammation [58]. Additionally, there are multiple mammalian chitinases that affect monocytic cells in chronic inflammatory and interact during osteoclastogenesis in pathological bone resorption [59]. This gene is decreased in palatal tissues of smokers [60] and with aging in periodontal ligament cells [61]. These are all consistent with the dysregulation of normal regulation of inflammatory responses with the onset of periodontal lesion formation.

This longitudinal study of disease initiation and progression in a human-like model of periodontitis provided some insights into the early lesion development at the molecular level that cannot be discerned from point-in-time human disease studies, and would be predicted to differ substantially from the host-microbial interactions that might occur in rodent disease models. The findings show clear patterns of macrophage features demarcated by gene expression patterns in the gingival tissues that were related to age and disease. Of interest within the macrophage gene clusters for the M0, M1, and M2 cells, the predominant distribution of samples with the M0 and M1 clusters appeared to be a reflection of the age of the animals. In contrast, the M2 cluster distribution reflected both age and time point of health, disease, or resolution of the gingival tissues. The outcomes enable a clearer definition of the kinetics and dynamics of macrophage infiltration, activation, and polarization in gingival tissues that should help explain the breakdown of homeostasis and gingival health and resulting changes that reflect a biological progression of tissue destruction. However, whether this macrophage polarization occurs prior to the emigration and infiltration process, or these phenotypic differentiation and maturation events occur once the monocytes/macrophages have successfully colonized the local tissues remain a gap in knowledge. Moreover, the

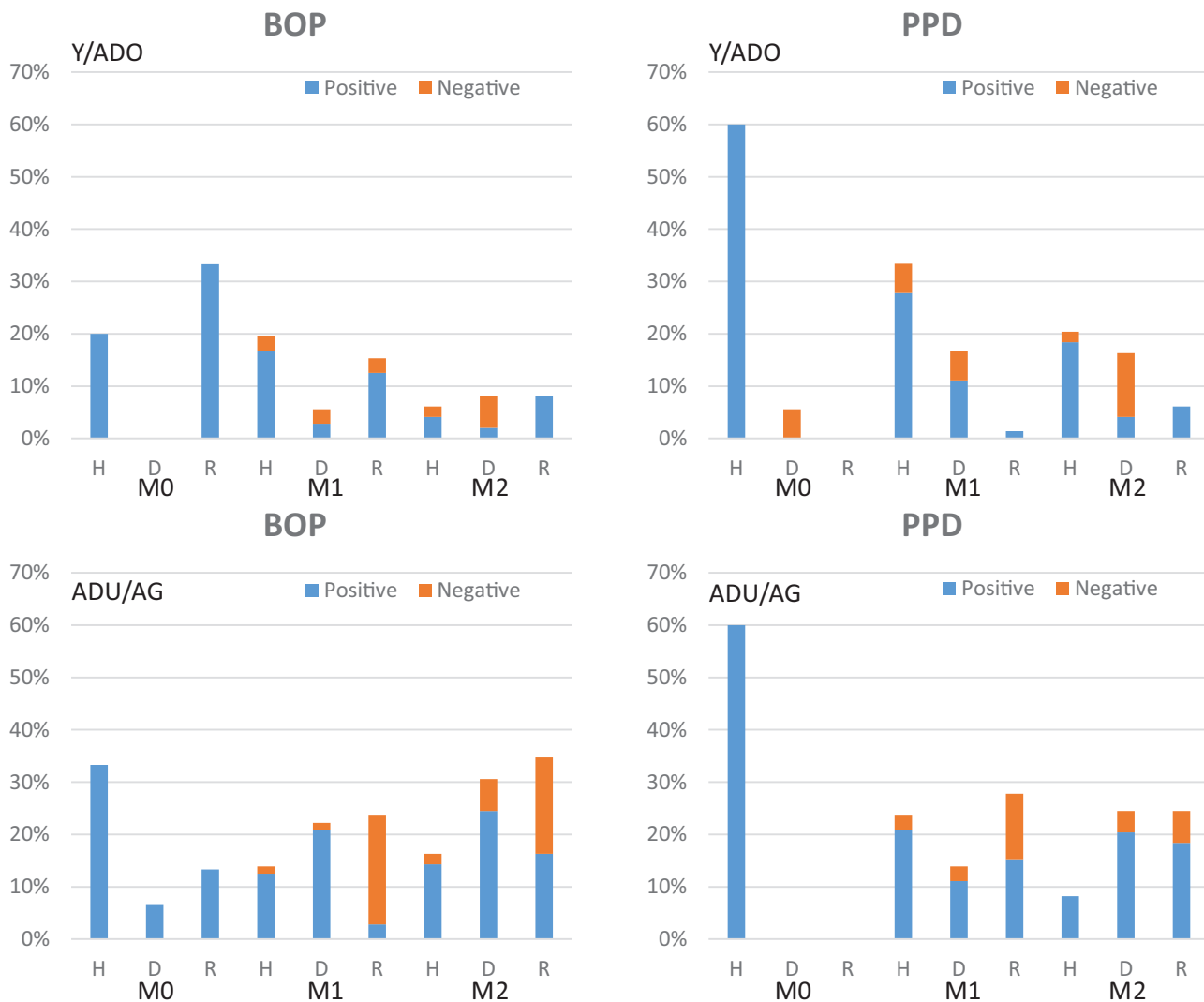


Figure 20: Display of the correlations between the macrophage genes and clinical disease features of BOP and PPD. The bars denote the frequency of significant ($P < 0.05$) positive and negative correlations with the macrophage genes.

occurrence, frequency, and activation signals in the tissues that alter the distribution of polarization, as well as modify the trajectory and direction of polarization have not been defined and could be critical for understanding disease biologic initiation, progression, and resolution.

Acknowledgements

We express our gratitude to the Caribbean Primate Research Center (CPRC) and the Microarray Core of University Kentucky, and Dr Arnold Stromberg for their invaluable technical assistance and initial management of the transcriptomic data.

Conflict of interests

The authors state no conflict of interest with any of the aspects of this study and report.

Funding

This work was supported by National Institute of Health grants P20GM103538 and UL1TR000117 to University

of Kentucky and P40RR03640 to the Caribbean Primate Research Center.

Data availability

The data have been uploaded into GEO accession GSE180588 (<https://www.ncbi.nlm.nih.gov/gds>).

Author contributions

O.A.G. and J.L.E. we responsible for the design and implementation of the study, collection of clinical data, interpretation of the transcriptomic data, preparing, and revising the report. S.S.K. was responsible for the preparation of samples, obtaining the microarray data, and preparation and review of the manuscript. L.M.N. was responsible for the statistical analyses, and preparation and review of the manuscript.

Animal research assurance

The methods were carried out in accordance with all relevant regulations for the use of nonhuman primates following ARRIVE guidelines.

References

1. Armitage GC. Learned and unlearned concepts in periodontal diagnostics: a 50-year perspective. *Periodontol 2000* 2013, 62, 20–36.
2. Wade WG. The oral microbiome in health and disease. *Pharmacol Res* 2013, 69, 137–43. doi:10.1016/j.phrs.2012.11.006.
3. Hajishengallis G. The inflammophilic character of the periodontitis-associated microbiota. *Mol Oral Microbiol* 2014, 29, 248–57.
4. Souza PP, Lerner UH. The role of cytokines in inflammatory bone loss. *Immunol Invest* 2013, 42, 555–622.
5. Hajishengallis E, Hajishengallis G. Neutrophil homeostasis and periodontal health in children and adults. *J Dent Res* 2014, 93, 231–7.
6. Scott DA, Krauss J. Neutrophils in periodontal inflammation. *Front Oral Biol* 2012, 15, 56–83.
7. Smith M, Seymour GJ, Cullinan MP. Histopathological features of chronic and aggressive periodontitis. *Periodontology* 2000 2010, 53, 45–54. doi:10.1111/j.1600-0757.2010.00354.x.
8. Cohen N, Morisset J, Emilie D. Induction of tolerance by *Porphyromonas gingivalis* on APCs: a mechanism implicated in periodontal infection. *J Dent Res* 2004, 83, 429–33. doi:10.1177/154405910408300515.
9. Cutler CW, Jotwani R, Palucka KA, Davoust J, Bell D, Banchereau J. Evidence and a novel hypothesis for the role of dendritic cells and *Porphyromonas gingivalis* in adult periodontitis. *J Periodontol Res* 1999, 34, 406–12. doi:10.1111/j.1600-0765.1999.tb02274.x.
10. Tanaka S, Fakher M, Barbour SE, Schenkein HA, Tew JG. Influence of proinflammatory cytokines on *Actinobacillus actinomycetemcomitans* specific IgG responses. *J Periodontol Res* 2006, 41, 1–9. doi:10.1111/j.1600-0765.2005.00829.x.
11. Papadopoulos G, Weinberg EO, Massari P, Gibson FC 3rd, Wetzler LM, Morgan EF, et al. Macrophage-specific TLR2 signaling mediates pathogen-induced TNF-dependent inflammatory oral bone loss. *J Immunol* 2013, 190, 1148–57.
12. Nanbara H, Wara-aswapati N, Nagasawa T, Yoshida Y, Yashiro R, Bando Y, et al. Modulation of Wnt5a expression by periodontopathic bacteria. *PLoS One* 2012, 7, e34434. doi:10.1371/journal.pone.0034434.
13. Zekha SA, Freilich RW, Amar S. Periodontal innate immune mechanisms relevant to atherosclerosis and obesity. *Periodontol 2000* 2010, 54, 207–21.
14. Cutler CW, Teng YT. Oral mucosal dendritic cells and periodontitis: many sides of the same coin with new twists. *Periodontol 2000* 2007, 45, 35–50.
15. Girardi M. Immunosurveillance and immunoregulation by gammadelta T cells. *J Invest Dermatol* 2006, 126, 25–31. doi:10.1038/sj.jid.5700003.
16. Gray EE, Cyster JG. Lymph node macrophages. *J Innate Immun* 2012, 4, 424–36. doi:10.1159/000337007.
17. Banchereau J, Briere F, Caux C, Davoust J, Lebecque S, Liu YJ, et al. Immunobiology of dendritic cells. *Annu Rev Immunol* 2000, 18, 767–811.
18. Ren L, Leung WK, Darveau RP, Jin L. The expression profile of lipopolysaccharide-binding protein, membrane-bound CD14, and toll-like receptors 2 and 4 in chronic periodontitis. *J Periodontol* 2005, 76, 1950–9. doi:10.1902/jop.2005.76.11.1950.
19. Cutler CW, Jotwani R. Antigen-presentation and the role of dendritic cells in periodontitis. *Periodontol 2000* 2004, 35, 135–57. doi:10.1111/j.0906-6713.2004.003560.x.
20. Locati M, Mantovani A, Sica A. Macrophage activation and polarization as an adaptive component of innate immunity. *Adv Immunol* 2013, 120, 163–84.
21. Mantovani A, Biswas SK, Galdiero MR, Sica A, Locati M. Macrophage plasticity and polarization in tissue repair and remodelling. *J Pathol* 2013, 229, 176–85.
22. Zhou D, Huang C, Lin Z, Zhan S, Kong L, Fang C, et al. Macrophage polarization and function with emphasis on the evolving roles of coordinated regulation of cellular signaling pathways. *Cell Signal* 2014, 26, 192–7.
23. Sica A, Mantovani A. Macrophage plasticity and polarization: in vivo veritas. *J Clin Invest* 2012, 122, 787–95. doi:10.1172/jci59643.
24. Gratchev A, Schledzewski K, Guillot P, Goerdts S. Alternatively activated antigen-presenting cells: molecular repertoire, immune regulation, and healing. *Skin Pharmacol Appl Skin Physiol* 2001, 14, 272–9.
25. Rodriguez M, Domingo E, Municio C, Alvarez Y, Hugo E, Fernandez N, et al. Polarization of the innate immune response by prostaglandin E2: a puzzle of receptors and signals. *Mol Pharmacol* 2014, 85, 187–97.
26. Martinez FO, Sica A, Mantovani A, Locati M. Macrophage activation and polarization. *Front Biosci* 2008, 13, 453–61.
27. Blach-Olszewska Z. Innate immunity: cells, receptors, and signaling pathways. *Arch Immunol Ther Exp (Warsz)* 2005, 53, 245–53.
28. Allavena P, Chieppa M, Monti P, Piemonti L. From pattern recognition receptor to regulator of homeostasis: the double-faced macrophage mannose receptor. *Crit Rev Immunol* 2004, 24, 179–92. doi:10.1615/critrevimmunol.v24.i3.20.
29. Striz I, Brabcova E, Kolesar L, Sekerkova A. Cytokine networking of innate immunity cells: a potential target of therapy. *Clin Sci (Lond)* 2014, 126, 593–612.
30. Zanoni I, Granucci F. Regulation and dysregulation of innate immunity by NFAT signaling downstream of pattern recognition receptors (PRRs). *Eur J Immunol* 2012, 42, 1924–31. doi:10.1002/eji.201242580.
31. den Haan JM, Kraal G. Innate immune functions of macrophage subpopulations in the spleen. *J Innate Immun* 2012, 4, 437–45. doi:10.1159/000335216.
32. Kawai T, Akira S. Innate immune recognition of viral infection. *Nat Immunol* 2006, 7, 131–7. doi:10.1038/ni1303.
33. Ferrante CJ, Leibovich SJ. Regulation of macrophage polarization and wound healing. *Adv Wound Care (New Rochelle)* 2012, 1, 10–6.
34. Schaible B, Schaffer K, Taylor CT. Hypoxia, innate immunity and infection in the lung. *Respir Physiol Neurobiol* 2010, 174, 235–43. doi:10.1016/j.resp.2010.08.006.
35. Salomao R, Brunialti MK, Rapozo MM, Baggio-Zappia GL, Galanos C, Freudenberg M. Bacterial sensing, cell signaling, and modulation of the immune response during sepsis. *Shock* 2012, 38, 227–42.
36. Hu L, Bray MD, Osorio M, Kopecko DJ. *Campylobacter jejuni* induces maturation and cytokine production in human dendritic cells. *Infect Immun* 2006, 74, 2697–705. doi:10.1128/iai.74.5.2697-2705.2006.
37. Hart AL, Al-Hassi HO, Rigby RJ, Bell SJ, Emmanuel AV, Knight SC, et al. Characteristics of intestinal dendritic cells in inflammatory bowel diseases. *Gastroenterology* 2005, 129, 50–65. doi:10.1053/j.gastro.2005.05.013.
38. Gervassi A, Alderson MR, Suchland R, Maisonneuve JF, Grabstein KH, Probst P. Differential regulation of inflammatory cytokine secretion by human dendritic cells upon *Chlamydia trachomatis* infection. *Infect Immun* 2004, 72, 7231–9. doi:10.1128/iai.72.12.7231-7239.2004.
39. Kranzer K, Eckhardt A, Aigner M, Knoll G, Deml L, Speth C, et al. Induction of maturation and cytokine release of human dendritic cells by *Helicobacter pylori*. *Infect Immun* 2004, 72, 4416–23. doi:10.1128/iai.72.8.4416-4423.2004.
40. Karlsson H, Larsson P, Wold AE, Rudin A. Pattern of cytokine responses to gram-positive and gram-negative commensal bacteria is profoundly changed when monocytes differentiate into dendritic cells. *Infect Immun* 2004, 72, 2671–8. doi:10.1128/iai.72.5.2671-2678.2004.
41. Guiney DG, Hasegawa P, Cole SP. *Helicobacter pylori* preferentially induces interleukin 12 (IL-12) rather than IL-6 or IL-10 in human dendritic cells. *Infect Immun* 2003, 71, 4163–6. doi:10.1128/iai.71.7.4163-4166.2003.
42. Ebersole JL, Steffen MJ, Gonzalez-Martinez J, Novak MJ. Effects of age and oral disease on systemic inflammatory and immune

- parameters in nonhuman primates. *Clin Vaccine Immunol* 2008, 15, 1067–75. doi:10.1128/cvi.00258-07.
43. Ebersole JL, Nagarajan R, Kirakodu S, Gonzalez OA. Transcriptomic phases of periodontitis lesions using the nonhuman primate model. *Sci Rep* 2021, 11, 9282.
44. Ebersole JL, Kirakodu S, Novak MJ, Stromberg AJ, Shen S, Orraca L, et al. Cytokine gene expression profiles during initiation, progression and resolution of periodontitis. *J Clin Periodontol* 2014, 41, 853–61.
45. Ebersole JL, Kirakodu SS, Gonzalez OA. Oral microbiome interactions with gingival gene expression patterns for apoptosis, autophagy and hypoxia pathways in progressing periodontitis. *Immunology* 2021, 162, 405–17. doi:10.1111/imm.13292.
46. Meka A, Bakthavatchalu V, Sathishkumar S, Lopez MC, Verma RK, Waller SM, et al. Porphyromonas gingivalis infection-induced tissue and bone transcriptional profiles. *Mol Oral Microbiol*, 2010, 25, 61–74.
47. Gonzalez OA, Stromberg AJ, Huggins PM, Gonzalez-Martinez J, Novak MJ, Ebersole JL. Apoptotic genes are differentially expressed in aged gingival tissue. *J Dent Res* 2011, 90, 880–6. doi:10.1177/0022034511403744.
48. Sun X, Gao J, Meng X, Lu X, Zhang L, Chen R. Polarized macrophages in periodontitis: characteristics, function, and molecular signaling. *Front Immunol* 2021, 12, 763334.
49. Momen-Heravi F, Friedman RA, Albeshri S, Sawle A, Keschull M, Kuhn A, et al. Cell type-specific decomposition of gingival tissue transcriptomes. *J Dent Res* 2021, 100, 549–56. doi:10.1177/0022034520979614.
50. Li W, Zhang Z, Wang ZM. Differential immune cell infiltrations between healthy periodontal and chronic periodontitis tissues. *BMC Oral Health* 2020, 20, 293.
51. Gonzalez OA, Novak MJ, Kirakodu S, Stromberg A, Nagarajan R, Huang CB, et al. Differential gene expression profiles reflecting macrophage polarization in aging and periodontitis gingival tissues. *Immunol Invest* 2015, 44, 643–64. doi:10.3109/08820139.2015.1070269.
52. Williams DW, Greenwell-Wild T, Brenchley L, Dutzan N, Overmiller A, Sawaya AP, et al. Human oral mucosa cell atlas reveals a stromal-neutrophil axis regulating tissue immunity. *Cell* 2021, 184, 4090–4104.e15. doi:10.1016/j.cell.2021.05.013.
53. Caetano AJ, Human Cell Atlas O, Craniofacial B, Sequeira I, Byrd KM. A roadmap for the human oral and Craniofacial Cell Atlas. *J Dent Res* 2022, 101, 1274–88.
54. Gonzalez OA, Novak MJ, Kirakodu S, Orraca L, Chen KC, Stromberg A, et al. Comparative analysis of gingival tissue antigen presentation pathways in ageing and periodontitis. *J Clin Periodontol* 2014, 41, 327–39. doi:10.1111/jcpe.12212.
55. Gonzalez OA, John Novak M, Kirakodu S, Stromberg AJ, Shen S, Orraca L, et al. Effects of aging on apoptosis gene expression in oral mucosal tissues. *Apoptosis* 2013, 18, 249–59. doi:10.1007/s10495-013-0806-x.
56. Ebersole JL, Nguyen LM, Gonzalez OA. Gingival tissue antibody gene utilization in aging and periodontitis. *J Periodontol Res* 2022, 57, 780–798. doi:10.1111/jre.13000.
57. Chang YC, Lai CC, Lin LF, Ni WF, Tsai CH. The up-regulation of heme oxygenase-1 expression in human gingival fibroblasts stimulated with nicotine. *J Periodontol Res* 2005, 40, 252–7. doi:10.1111/j.1600-0765.2005.00804.x.
58. Ren J, Han X, Lohner H, Liang R, Liang S, Wang H. Serum- and Glucocorticoid-Inducible Kinase 1 promotes alternative macrophage polarization and restrains inflammation through FoxO1 and STAT3 signaling. *J Immunol* 2021, 207, 268–80. doi:10.4049/jimmunol.2001455.
59. Di Rosa M, Tibullo D, Vecchio M, Nunnari G, Saccone S, Di Raimondo F, et al. Determination of chitinases family during osteoclastogenesis. *Bone* 2014, 61, 55–63. doi:10.1016/j.bone.2014.01.005.
60. Wang Y, Anderson EP, Tatakis DN. Whole transcriptome analysis of smoker palatal mucosa identifies multiple downregulated innate immunity genes. *J Periodontol* 2020, 91, 756–66. doi:10.1002/jper.19-0467.
61. Johnson AA, Shokhirev MN. Pan-tissue aging clock genes that have intimate connections with the immune system and age-related disease. *Rejuvenation Res* 2021, 24, 377–89. doi:10.1089/rej.2021.0012.